Catalysis Communications 180 (2023) 106707

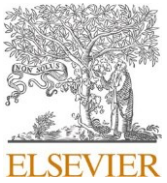

Contents lists available at ScienceDirect

Catalysis Communications

journal homepage: www.elsevier.com/locate/catcom

Transient responses of product formation in nonthermal plasma-assisted D_2O-CO_2-rubber reaction

Steven S.C. Chuang [a,*], Fnu Huhe [a], Aderinsola Oduntan [a,b], Zhenmeng Peng [c]

[a] School of Polymer Science and Polymer Engineering, 44325-3909, United States of America
[b] Department of Chemical and Biomolecular Engineering, The University of Akron, Akron, OH 44325-3909, United States of America
[c] Department of Chemical Engineering, The University of South Carolina, Columbia, SC 29208, United States of America

ARTICLE INFO

Keywords:
Nonthermal plasma
Nickel
Deuterium
Rubber
Hydrogen production
Reforming reaction
Transient kinetics

ABSTRACT

Nonthermal plasma-assisted reactions at ambient temperature hold promise for applications in upcycling of polymer wastes. Transient studies showed that the H_2 response led that of D_2, indicating that C−H breaking occurred earlier than D-OD bond breaking in D_2O-rubber and D_2O-CO_2-rubber reactions. The CH_4 response led that of C_2H_6, indicating that Ni-based catalyst is highly favorable for catalyzing the formation of CH_4. CO_2 plasma produced oxygen which could oxidize part of CH_4 and C_2H_6 from rubber. This study demonstrated that the transient kinetic (response) method, for the first time, is effective in producing data for elucidating mechanisms of nonthermal plasma-assisted catalysis.

1. Introduction

Upcycling polymer wastes to useful compounds in a cost-effective manner is highly challenging because these processes are highly energy intensive with low selectivity toward desirable products [1,2]. Extensive thermal and catalysis research efforts have shown that the reactions involved with hydrocarbon such as methane or polymers at temperatures above 300 °C often led to the formation of coking and tar (a high molecular aromatic species) on either the reactor's wall or catalyst's surface, presenting many significant problems in product separation, reactor operation, and its associated cost [3]. The problems of coking and tar formations as well as low selectivity may be alleviated by operating the reaction processes at low temperatures if the rates of the desirable reactions can be accelerated. Thus, we had attempted to use nonthermal dielectric barrier discharge (DBD) plasma to initiate catalytic hydrogenolysis of polystyrene and polyethylene to gaseous $C_1 - C_3$ hydrocarbons at temperatures below 100 °C [4,5]. A selective conversion of polymers to C_2 or C_3 olefins initiated by DBD plasma is technically feasible at temperatures significantly lower than those used in thermal catalytic processes.

It is instructive to briefly describe the distinction between thermal and nonthermal plasma [6]. In thermal plasma, temperatures of charged particles (ions), noncharged particles (including atoms, molecules, and radicals), and electrons are the same, indicating that all species are at thermal equilibrium. In contrast, the temperatures of electrons in nonthermal plasma are in 10^4–10^5 K which are several orders of magnitude higher than those in the charged particles [7]. Non thermal DBD plasma could have their charged particles at ambient temperature or slightly higher. Because charged particles contain low thermal energy, it takes significantly less energy to produce nonthermal plasma than thermal plasma.

In a nonthermal dielectric barrier discharge (DBD) plasma-initiated reaction process, a fixed amount of electric energy in the form of the AC voltage-induced dielectric barrier discharge is applied to the reactor, which is packed with a dielectric material, to produce charged particles and electrons from the species in the gas phase. Then, gaseous charged species (i.e., positive ions and electrons) initiate a bond-breaking process such as C−H bond breaking in hydrocarbons (methane or polymers), the H−H bond breaking in hydrogenolysis, and the H−O bond breaking in H_2O in steam reforming, and the C−O bond breaking in CO_2 dry reforming reaction [8–10].

We expect that the amount of electric power for initiating H_2-plasma in the hydrogenolysis of polymer would be in the same range as those reforming reactions initiated with H_2O and CO_2 plasma. We are interested in using H_2O and CO_2 instead of H_2 because of the cost, the safety, and the potential for converting H_2O and CO_2 with polymer to H_2, CO, and C_1-C_3 hydrocarbons, especially ethylene. DBD could produce a spark which denotates combustion of fuels with oxygen if sufficient amounts

* Corresponding author.
E-mail address: schuang@uakron.edu (S.S.C. Chuang).

https://doi.org/10.1016/j.catcom.2023.106707
Received 1 March 2023; Received in revised form 28 May 2023; Accepted 29 May 2023
Available online 2 June 2023

of hydrogen and oxygen are available. DBD has been studied for CO_2-H_2O reaction, steam reforming and CO_2 reforming reactions over oxide-supported metal and metal oxide catalysts. The results suggest that catalysts might be used to modify the reaction pathways of intermediates generated from the plasma-initiated gas phase reactions.

In this study, we report results of a preliminary study on the DBD-plasma-initiated reforming reaction of rubber with CO_2 and H_2O over a Ni (Nickel)-based catalyst. Ni was used because it is known to exhibit catalytic activities for both thermal catalytic and plasma-initiated steam and dry-reforming of methane (CO_2-CH_4) reactions, and hydropyrolysis of polycarbonate [11–13]. These studies suggested that Ni possesses activities for breaking C−O, C−H and C−C bonds and forming H−H bonds. Transient responses of product formation recorded after a step change in the composition of gas flow and a pulse mode of AC electric power imposed have shown that H_2 evolved earlier than HD/D_2 and CH_4 evolved earlier than C_2H_6. The results of these transient studies were used for elucidating some important steps in the reaction pathways.

2. Experimental

The experimental setup of the non-thermal DBD plasma reactor and reaction test system are provided in **Fig. S1** (Supporting Information). The non-thermal DBD plasma reactor consisted of a cylindrical quartz tube (13 mm O.D. × 11.5 mm I.D.), a ground electrode (a copper rod with diameter of 40 mm, length of 100 mm, placed along the axis of the quartz tube), and a high voltage electrode (a copper tape wrapped around the outer surface of the tube). The discharge length of the DBD reactor was 50 mm. For each experiment, 1 g of rubber in powder form (particle size of 400 μm) was packed into the discharge space (between the ground electrode and the reactor body). The rubber was a standard raw material from MRP-PolyDyne. All experiments were carried out at atmospheric pressure and ambient temperature, ca. 25 °C. The AC power for driving nonthermal DBD plasma generator was supplied by PVM500–2500 with a voltage range of 6 kV to 9 kV, and a frequency range of 50–60 Hz. A 30 cm^3/min pure CO_2 gas stream was used for the CO_2-rubber reaction, whereas a 30 cm^3/min Ar gas after passed through a D_2O saturator was used for the D_2O-rubber reaction. The D_2O concentration in the Ar gas stream was around 2.5 vol%.

A transient kinetic experiment was designed and conducted by applying a perturbation to the reaction system and monitoring the product responses with online mass spectrometer. The perturbation included the following: (i) a step change in applying AC voltage and carrier gas concentration, and (ii) a pulse change in AC voltage. The composition of the reactor's effluent gas stream was monitored by a mass spectrometer, MS (OmniStar™ GSD 320 Gas Analysis System) and by an IR cell for identification of CO_2, CO, methane, and ethylene. Since the m/z (the ratio of mass to charge) for some of the ion fragments of CH_4, C_2H_4, C_2H_6, O_2, CO, and CO_2 are overlapped, we selected the m/z = 15 for CH_4, m/z = 16 for O_2, m/z = 28 for CO, m/z = 30 and 29 for C_2H_6. Note that the ion fragments of CO_2 at m/z = 29 ($^{13}CO^+$), 28 ($^{12}CO^+$), and 16 (O^+) was found to be less than 10% of m/z = 44 (use of CO_2/Ar gas mixture). The majority of m/z = 16, m/z = 28, and m/z = 29 signals was due to O_2, CO, and C_2H_6, respectively. In addition, these m/z ratios exhibited different profiles (i.e., intensity vs. time), allowing their unambiguous assignment. The effluent stream from the reactor was also directed to an infrared cell (IR gas detector) to obtain infrared spectra of gaseous products. Infrared spectroscopy provided distinct spectra for CO, CO_2, methane, ethylene, and ethane. In a CO- and O_2-free gas stream, we selected m/z = 16 for methane, m/z = 28 for C_2H_4, and m/z = 30 for C_2H_6. The concentration of specific gas product was obtained by calibration of the MS signal and IR band intensity through injecting a known amount of that species into the Ar gas flow at the same flow rate as that used in reaction studies. Some of the calibration results are shown in **Figs. S2** and **S3**.

The Ni-based catalyst was prepared by electrodeposition of Ni nitrate on a stainless-steel grid (a total surface area = 24 cm^2) as shown in Fig. S1, which was placed in an off-center position of the reactor in contact with rubber particles in the plasma zone.

3. Results and discussion

Fig. 1**(a)-(b)** shows a qualitative picture of the transient responses of CO, O_2, CH_4 and C_2H_6 recorded after applying the step change in AC electric field and then switching the inlet gas flow from Argon (Ar) to CO_2 in a step mode, where the Ar gas flow was replaced by the CO_2 gas flow. Turning on the AC electric field led to an immediate increase in H_2 followed by CH_4 and C_2H_6 (Fig. 1a). The presence of adsorbed water on the rubber, catalyst, and the reactor's wall provided oxygen for the formation of CO_2 and CO. The amounts of CO_2 and CO were removed from the reaction zone by purging the reactor with flowing Ar for a long period of time (more than 2.5 min.) before the step-switching of the flow from Ar to CO_2 was made. (see MS signals under Ar flow, Fig. 1a). Note that a step gas concentration switch was not performed accurately given the small disruption in the CO_2 flow, resulting in an uneven rising of CO_2 signal profile as shown in Fig. 1a. The responses of the CO and O_2 followed closely those of CO_2 (see Fig. 1(a), while H_2, CH_4, and C_2H_6 reached a maximum (see Fig. 1(b)), followed by a slight decline and then levelling off when the CO_2 concentration obtained was about 10%. Such a decline in responses could be attributed to the oxidation of H_2, CH_4, and C_2H_6 by oxygen produced from the CO_2 dissociation.

Comparison of the product responses depicted in Fig. 1b reveals the following order of appearance in time: $H_2 \rightarrow CH_4 \rightarrow C_2H_6$, reflecting the relative kinetic rates of their formation. Infrared results shown in **Fig. S4** and the compositions of rubber provided by the source showed that the rubber contains mainly CH_2 and C−C in its backbone and methyl side chain. Evidently, CO_2 plasma is more effective than Ar plasma in producing CH_4 and C_2H_6. Although the nature of adsorbed species on catalyst surface is unclear, we proposed a reaction pathway to explain the sequence of product formation shown in Scheme 1. CO_2 and/or H_2O plasma contain various forms of positive charged particles and electrons which initiated the C−H bond breaking on CH_2, leading to the following sequence: (i) formation of H_2, (ii) breaking of C−C bond of the side CH_3 resulting in CH_4 formation, and (iii) subsequent C−C bond breaking resulting in the formation of a C_2-hydrocarbon species, i.e., C_2H_6.

The rubber reaction could begin with C−H bond breaking on a secondary C because it has the lowest C−H bond energy in the rubber. Following C−H breaking, we would expect C−C bond breaking since it has the lowest bond energy in the entire rubber structure. We were not able to determine if the fragments of rubber are in the form of radical or charged species. However, we speculate that the adsorbed species on the Ni-based catalysts could be in the form of radical species because the catalysts may not carry electric charge and they are connected to an electric power source. Ni-based catalysts in the reactor may play a role in the formation of H_2, CH_4, and C_2H_6 through adsorption of the fragments of rubber in the gas phase, followed by hydrogenation and desorption process steps. These steps on the Ni catalyst surface or on the surface of reactor wall could be the key reason why the transient response of the H_2, HD, CH_4, and C_2H_6 occurred on a time scale of seconds. Further studies will be made by varying the amount of Ni catalysts and measuring the product responses as well as controlling the surface structure of Ni catalysts.

Continuous application of 9 kV AC electric field resulted in a gradual increase in the temperature of reactor. Thus, we switched the mode of applying AC electric field from a continuous mode to a pulse mode which lasted for 6 s. The responses are shown in **Fig. S5**. The products produced from the pulse responses were the same as those from step switching from Ar flow to CO_2 gas flow. However, the lead/lag relationship for the product formation cannot be clearly discerned. This resulted from the use of pure CO_2 gas flow which produced a significant quantity of O_2. Oxygen further oxidizes the gaseous products, blurring their lead/lag responses. The step switch mode shown in Fig. 1 allowed us to observe the lead/lag responses of products at the point where CO_2

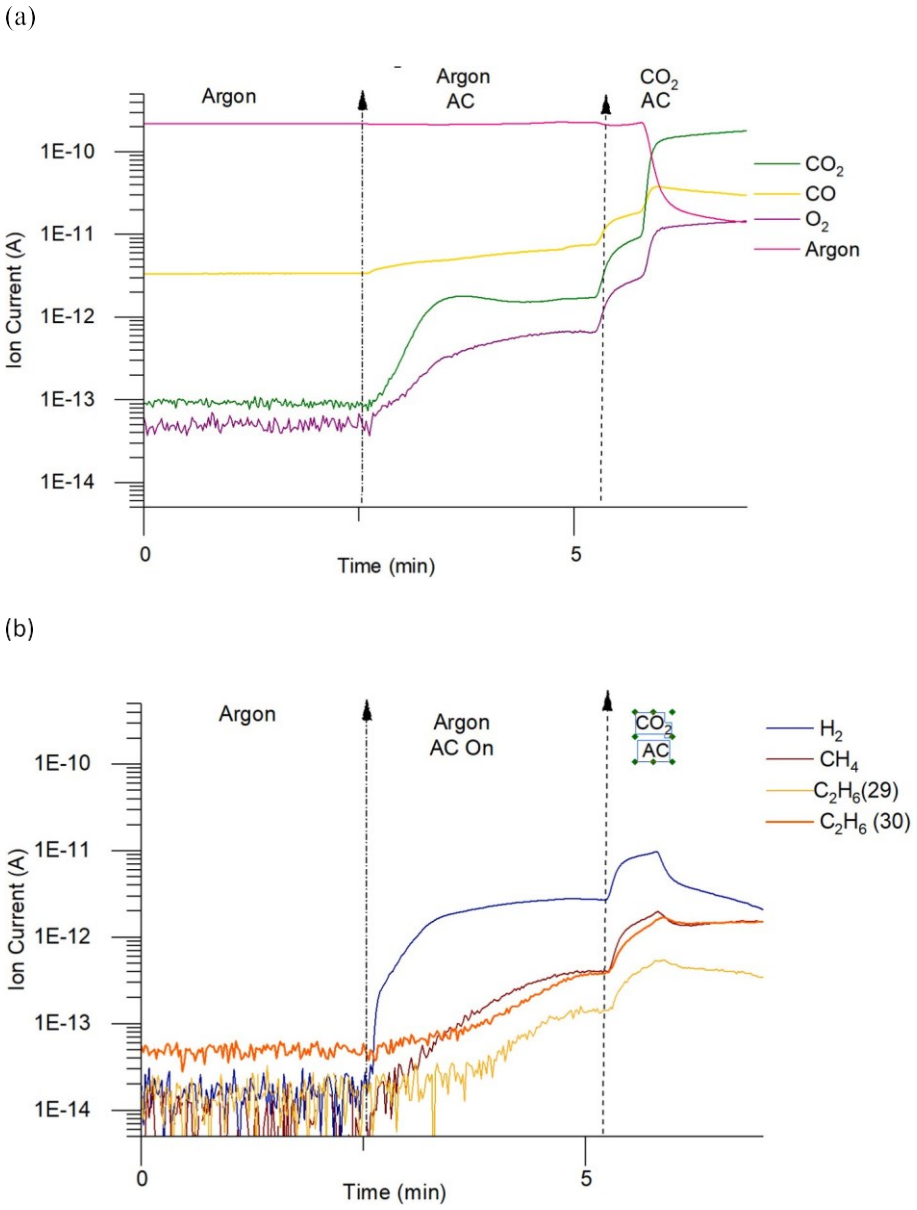

Fig. 1. Flowing 30 cm^3/mm of Ar over 1 g rubber, turning on the 9 kV AC electric field at 2.5 min, and switching from Ar to CO_2 flow at 5.1 min. (a) CO_2, CO_2, O_2, and Ar responses and (b) H_2, CH_4, and C_2H_6 responses.

concentration is below 10%, and a significant amount of oxygen for oxidation had not yet been produced.

Fig. 2 shows the transient response of products resulting from applying 20 s of 6 kV AC to generate plasma during the flow of D_2O/CO_2 over 1 g of rubber. The amounts of products formed were determined using calibration curves as shown in Fig. S3. The transient profiles depicted in Fig. 2 show that the formation of H_2 slightly led that of HD. By increasing the AC voltage from 6 to 9 kV the formation of H_2 was increased. The amount of D_2 (not shown in Fig. 2) produced is significantly less than that of H_2 and HD. Both H_2 and HD isotope gas are major products, indicating that the presence of D_2O facilitated C−H bond breaking in the rubber. The formation of CH_4 and C_2H_6 revealed that the C−C bond breaking was initiated by the application of CO_2/D_2O plasma. As illustrated in Scheme 1, the C−H bond breaking led to the cracking of the C−C backbone in the rubber structure, and as a result of this ethane gas product was formed.

The transient response of the Ar/D_2O-rubber reaction to the application of 20-s duration AC power is shown in Fig. 3, where the formation of products proceeded in the following sequence: H_2, CH_4, CO_2, HD, and D_2. CO_2 had also been observed as a major product in nonthermal plasma methane reforming reaction. The CO_2 response suggests that OD resulting from the presence of D_2O served as oxidant to oxidize fragments of rubber to produce CO_2. In addition, OD· (radical) and CO could further react to produce CO_2 and D (adsorbed species). The slow response of D_2 gas indicates combination of two adsorbed D species is a slow step, which could be due to kinetic isotope effects [14,15]. We expect that the sequence of the evolution of the H_2, CH_4, and C_2H_4 for the D_2O-rubber and CO_2/D_2O-rubber reactions follow the reaction pathway depicted in Scheme 1. The key difference is that D_2O/CO_2 plasma produced more CH_4 than the D_2O/Ar plasma.

4. Conclusions

The transient response method coupled with the use of isotope gas (D_2O) was applied to investigatingthe nonthermal plasma-initiated D_2O/CO_2-rubber reaction over a Ni-based catalyst at ambient temperature. The most significant observation was that the H_2 response led that of D_2 and the CH_4 response led that of C_2H_6, demonstrating that the

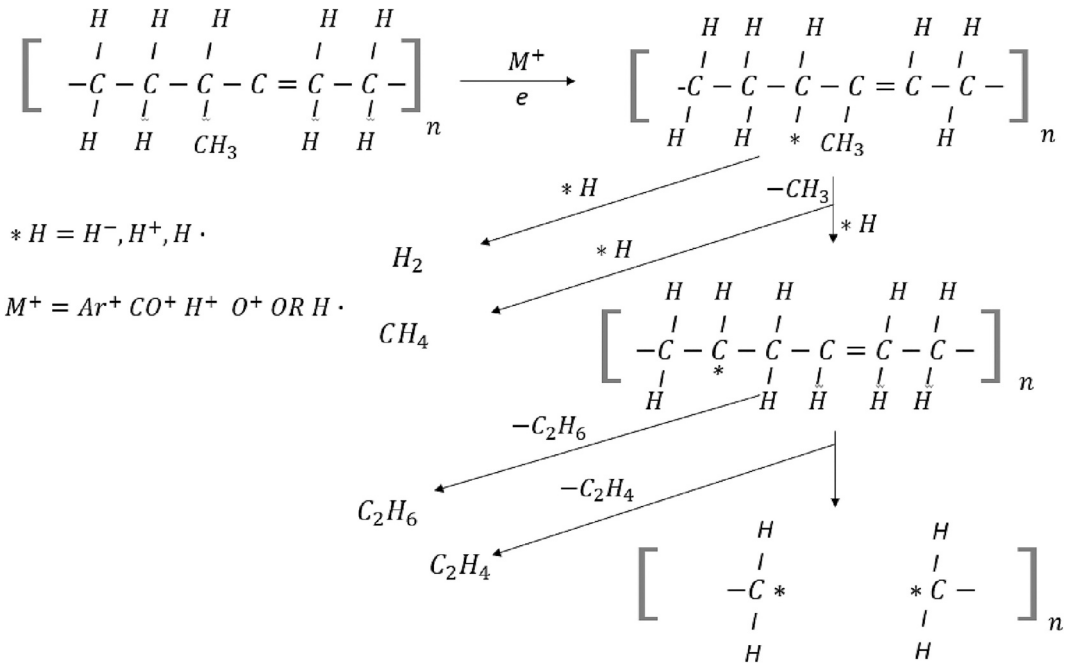

Scheme 1. Proposed reaction pathway of rubber decomposition with nonthermal plasma; * represents a charged species or a free radical.

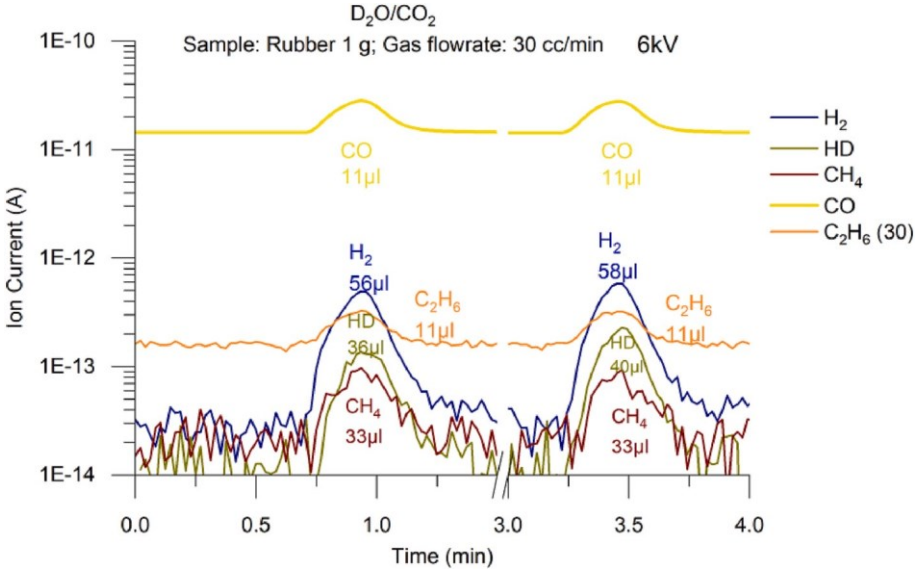

Fig. 2. Transient responses of products resulting from applying for 20 s 6 kV AC in the flow of D_2O/CO_2 over 1 g rubber. D_2O was brought into the feed line by passing 30 cc/min of CO_2 through a saturator filled with D_2O. D_2 response is not shown (very noisy because of the low quantity formed).

transient response method was effective in studying the mechanism of nonthermal plasma-initiated reactions on a time scale of seconds at ambient temperature. Since the bond-breaking and bond-formation processes in a gas-phase homogeneous reaction occur on a time scale of less than nanoseconds, the observed transient responses on the time scale of seconds suggest that the formation of the gaseous products H_2, HD, D_2, CO, O_2, CH_4, C_2H_4, and C_2H_6, involves adsorption, surface reaction, and desorption steps. One of these reaction steps could occur on a time scale of seconds, slowing down the overall process for the formation of gaseous products.

Ar, CO_2, D_2O/Ar, D_2O/CO_2-nonthermal plasma initiated the bond breaking process in the rubber solid material to a different extent, producing desirable products: H_2, CH_4, C_2H_4, and C_2H_6. D_2O tracing studies showed that H_2 produced from C−H bond breaking in the rubber occurred prior to the D-OD bond breaking. In other words, a nonthermal steam reforming of hydrocarbon would produce more hydrogen at high rates from hydrocarbons than from water. The presence of CO_2 can enhance the formation of methane. However, CO_2 plasma also produced oxygen which can further oxidize the desirable products.

In addition to the types of catalysts, the voltage and frequency of electric field, the type of gas and mixed gases, electrode arrangements, and flow rate played a role in the reaction process. Nonthermal DBD and plasma-assisted catalysis are still at an infant stage [16]. Much work remains to be done on improving the contact between catalyst and rubber particles, determining the role of diffusion on the rate of primary and secondary product formation as well as identifying the catalyst composition/structure for enhancing the selectivity and yields of desirable products.

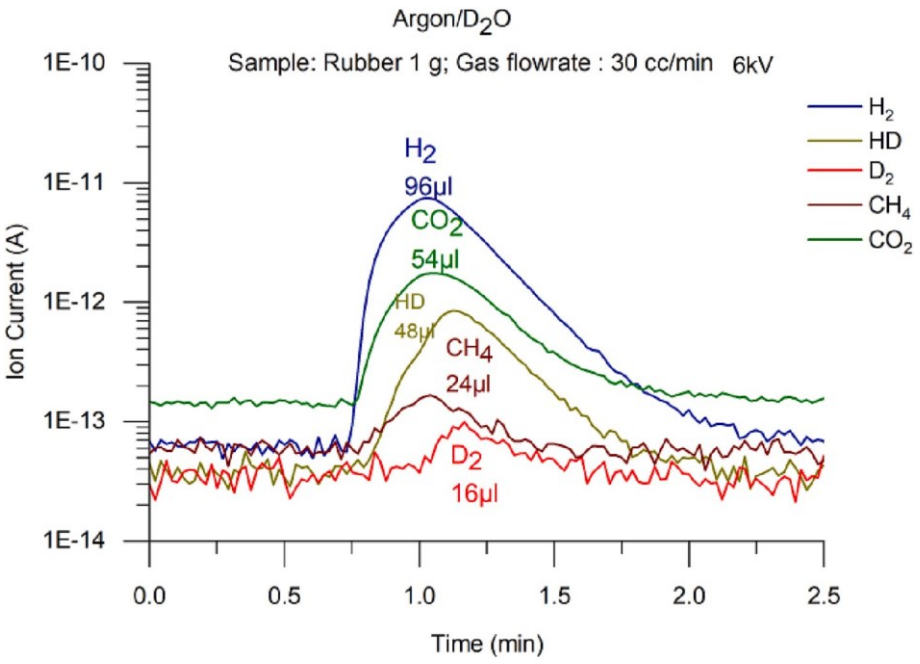

Fig. 3. Transient responses products resulting from applying 20 s of 6 kV AC ring flowing 30 cc/min of Ar/D_2O over 1 g rubber.

Credit author statement

Steven S.C Chuang

- Organized literature, designed experiments, provided the approaches for data analysis, and interpretation of data.
- Wrote the draft, revised, and finalized manuscript.

FNU Huhe

- Carried out the experimental study and plotted results.

Aderinsola Oduntan

- Assist in data analysis and plotting Figures.

Zhenmeng Peng

- Provided nonthermal plasma dielectric barrier approaches and initial reactor design.

Declaration of Competing Interest

The authors declare the following financial interests/personal relationships which may be considered as potential competing interests:

Aderinsola Oduntana reports financial support was provided by The University of Akron. Zhenmeng Peng reports equipment, drugs, or supplies was provided by The University of Akron.

Data availability

Data will be made available on request.

Acknowledgements

This work was supported by the financial support of the U.S. National Science Foundation (Grant No. 2132178).

Valuable comments from Prof. Angelos M Efstathiou are highly appreciated.

Appendix A. Supplementary data

Supplementary data to this article can be found online at https://doi.org/10.1016/j.catcom.2023.106707.

References

[1] X. Chen, Y. Wang, L. Zhang, Recent progress in the chemical upcycling of plastic wastes, ChemSusChem 14 (2021) 4137–4151.
[2] J. Huang, A. Veksha, W.P. Chan, A. Giannis, G. Lisak, Chemical recycling of plastic waste for sustainable material management: a prospective review on catalysts and processes, Renew. Sust. Energ. Rev. 154 (2022), 111866.
[3] A. Bin Jumah, V. Anbumuthu, A.A. Tedstone, A.A. Garforth, Catalyzing the hydrocracking of low density polyethylene, Ind. Eng. Chem. 58 (2019) 20601–20609.
[4] L. Yao, J. King, D. Wu, S.S. Chuang, Z. Peng, Non-thermal plasma-assisted hydrogenolysis of polyethylene to light hydrocarbons, Catal. Commun. 150 (2021), 106274.
[5] L. Yao, J. King, D. Wu, J. Ma, J. Li, R. Xie, S.S.C. Chuang, T. Miyoshi, Z. Peng, Non-thermal plasma-assisted rapid hydrogenolysis of polystyrene to high yield ethylene, Nat. Commun. 13 (2022) 885.
[6] A. Fridman, Plasma Chemistry, Cambridge University Press, New York, 2008.
[7] S. Li, X. Dang, X. Yu, G. Abbas, Q. Zhang, L. Cao, The application of dielectric barrier discharge non-thermal plasma in VOCs abatement: a review, Chem. Eng. J. 388 (2020), 124275.
[8] P. Mehta, P. Barboun, D.B. Go, J.C. Hicks, W.F. Schneider, Catalysis enabled by plasma activation of strong chemical bonds: a review, ACS Energy Lett. 4 (2019) 1115–1133.
[9] A. Bogaerts, E.C. Neyts, Plasma technology: an emerging Technology for Energy Storage, ACS Energy Lett. 3 (2018) 1013–1027.
[10] E.C. Neyts, K. Ostrikov, M.K. Sunkara, A. Bogaerts, Plasma catalysis: synergistic effects at the nanoscale, Chem. Rev. 115 (2015) 13408–13446.
[11] M.A. Vasiliades, C.M. Damaskinos, P. Djinovi´c, A. Pintar, A.M. Efstathiou, Dry reforming of CH_4 over $NiCo/Ce_{0.75}Zr_{0.25}O_{2-\delta}$: the effect of co on the site activity and carbon pathways studied by transient techniques, Catal. Commun. 149 (2021), 106237.
[12] Y. Zhang, J. Jiang, J. Wu, M. Wen, J. Wang, Upcycling waste polycarbonate plastics into jet fuels over NiCo/C by catalytic tandem hydropyrolysis/hydrodeoxygenation, Fuel Process. Technol. 247 (2023), 107809.
[13] K. Stanley, S. Kelly, J.A. Sullivan, Effect of Ni NP morphology on catalyst performance in non-thermal plasma-assisted dry reforming of methane, Appl. Catal. B 328 (2023), 122533.
[14] J. Happel, Isotopic Assessment of Heterogeneous Catalysis, Elsevier, 2012.
[15] M.A. Brundage, S.S.C. Chuang, Dynamic multiple tracing with D_2 and C_2D_4 in ethylene hydroformylation over $Mn\text{-}Rh/SiO_2$, J. Catal. 174 (1998) 164–176.
[16] B. Tabu, K. Akers, P. Yu, M. Baghirzade, E. Brack, C. Drew, J.H. Mack, H.-W. Wong, J.P. Trelles, Nonthermal atmospheric plasma reactors for hydrogen production from low-density polyethylene, Int. J. Hydrog. Energy 47 (2022) 39743–39757.